Photochemically- and Thermally-Generated BN-Doped Borafluorenate Heterocycles via Intramolecular Staudinger-Type Reactions

Bi Youan E. Tra,[a] Andrew Molino,[b] Kimberly K. Hollister,[a] Samir Kumar Sarkar,[a] Diane A. Dickie,[c] David J. D. Wilson,[b] Robert J. Gilliard, Jr.*[a]*

[a] Department of Chemistry, Massachusetts Institute of Technology, 77 Massachusetts Avenue, Building 18-596, Cambridge, MA 02139-4307, United States

[b] Department of Chemistry, La Trobe Institute for Molecular Science, La Trobe University, Melbourne, 3086, Victoria, Australia

[c] Department of Chemistry, University of Virginia, Charlottesville, Virginia 22904, United States

ABSTRACT

A series of BN-incorporated borafluorenate heterocycles, bis(borafluorene-phosphinimine)s (**11-15**) have been formed via *intra*molecular Staudinger-type reactions. The reactions were promoted by light or heat using monodentate phosphine-stabilized 9-azido-9-borafluorenes (R_3P-BF-N_3) (**6-10**) and involve the release of dinitrogen (N_2), phosphine migration from boron to nitrogen, and oxidation of the phosphorus center (P^{III} to P^{V}). Density functional theory (DFT) calculations provide mechanistic insight into the formation of these compounds. Compounds **11**-**15** are blue emissive in the solution and solid states with absolute quantum yields (Φ_F) ranging from 12-68%.

Introduction

Amongst boron-containing polycyclic aromatic hydrocarbons (PAH), 9-borafluorenes and their derivatives have become important small-molecule platforms for the construction of higher-value boracycles with unique reactivity trends, electronic features, and photophysical properties.[1-8] Research efforts in this regard have engaged a broad array of synthetic chemists interested in fundamental chemical transformations,[9-25] as well as those concerned with uncovering new types of functional materials.[3, 26-37] Recently, our laboratory synthesized a series of borafluorene radicals,[38] cations,[39, 40] and anions,[41-45] all of which rely on the key reaction of a neutral carbon donor ligand (Lewis base) and 9-bromo-9-borafluorene (Lewis acid). Reaction of the 9-carbene-9-borafluorene anion with carbon dioxide (CO_2) resulted in the formation of a trioxaborinanone, which releases carbon monoxide (CO) to form a luminescent dioxaborinanone (Figure 1A).[43] The carbene adduct of 9-phosphaketenido-9-borafluorene also loses CO under photochemical conditions to afford a BP-doped six-membered ring via a putative phosphinidene intermediate (Figure 1B).[46] The synthesis of these B- and BP-centered PAHs via the extrusion of a gaseous small-molecule inspired us to explore possible synthetic strategies to obtain related BN analogues.

Pioneering work by Bettinger and coworkers on the reaction chemistry of the parent 9-azido-9-borafluorene and its cyclic trimer led to the experimental realization of various BN-heterocycles (Figure 1C).[47-49] While the thermolysis of 9-azido-9-borafluorene yields a BN-cyclic tetramer, trapping reactions with trimethylsilyl chloride produces a monomeric BN-phenanthrene.[48] He[50] and Martin[51] have independently performed reactions of 9-aryl-9-borafluorenes and external organic azides which undergo N-insertion reactions, also giving BN-phenanthrenes (Figure 1D). Stephan has reported a series of phosphinimine-substituted boranes which are isolated when

azidocyclohexylborane reacts with trisubstituted phosphines via release of dinitrogen (Figure E).[52] We hypothesized that a ligand-mediated approach to 9-azido-9-borafluorene chemistry would lead to distinct BN-heterocycles via loss of dinitrogen (N_2) as the presence of the Lewis base has the potential to block or attenuate oligomerization. Herein, we report the synthesis, molecular structures, and optical properties of BN-incorporated borafluorenates, which have been obtained by photolysis and/or thermolysis of phosphine-complexed borafluorene azides (Figure 1F). Notably, these reactions represent rare instances of *intra*molecular Staudinger-type reactions. Theoretical mechanistic studies were carried out to model reaction pathways of the observed products.

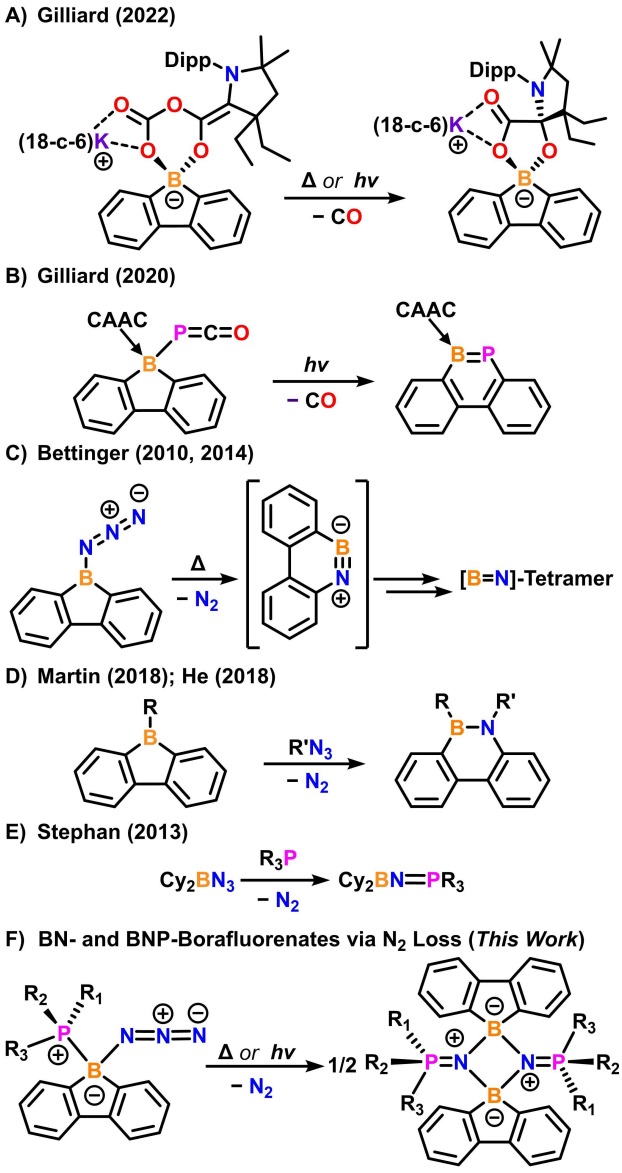

Figure 1. (A) Thermal or photolytic CO release from boraspirocycles; (B) Photolysis of 9-phosphaketenido-9-borafluorene promotes loss of CO; (C) Thermolysis of 9-azido-9-borafluorene yields a BN-cyclic tetramer via N_2 release; (D) Intermolecular reactions between 9-aryl-9-borafluorenes and organic azides produce BN-phenanthrenes via loss of N_2; (E) Synthesis of phosphinimine-substituted boranes via N_2 release; (F) This work: synthesis of BN-doped borafluorenates via N_2 loss.

Results and Discussion

Our ligand-based strategy toward BN-heterocycles began by exploring the chemistry of carbene-coordinated 9-azido-9-borafluorenes. However, these attempts led to complicated reactions which often produced protonated carbene at elevated temperatures. Employing a phosphine base instead of standard carbenes resulted in drastic differences in reactivity. A series of phosphine-supported 9-bromo-9-borafluorenes **1**-**5** were readily prepared in 92-96% yield (see supporting information for details).[35] Compounds **1**-**5** were reacted with trimethylsilyl azide (TMS-N_3) to afford the corresponding phosphine-stabilized 9-azido-9-borafluorenes **6-10** as white solids in 93-98% isolated yields (Scheme 1). Compounds **6-10** show strong absorption bands in the 2095-2105 cm^{-1} range corresponding to the -N_3 asymmetric stretching vibrations, which are comparable to the pyridine- and t-butyl pyridine-stabilized azido-borafluorene compounds reported by Bettinger (2125 and 2116 cm^{-1}, respectively).[47] Adducts **6-10** were characterized via X-ray crystallography (Figure 2). The boron centers adopt four-coordinate tetrahedral geometry. The boron-nitrogen ($B1–N_{azide}$) bond distances range from 1.5490(17)-1.574(6) Å and are similar to the B–N bond distances in the pyridine- and carbene-azido-borafluorenes (1.548(16)-1.572(3) Å).[47, 53]

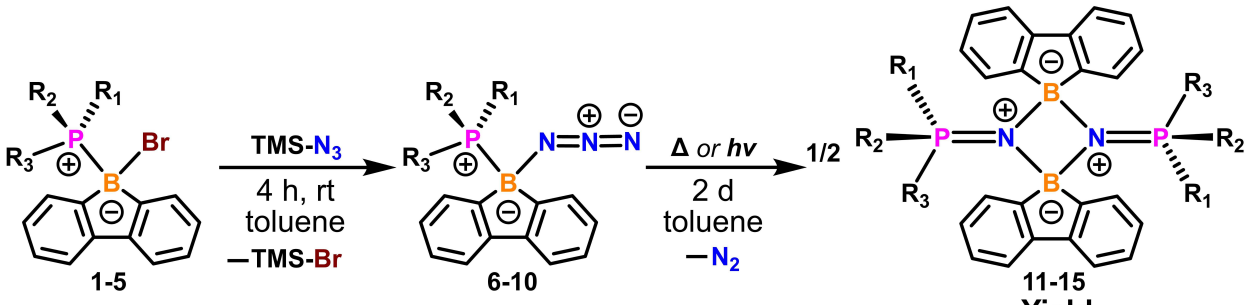

	Yield		Yield	
			Δ	*hv*
(1) $R_1 = R_2 = R_3$ = Me	**(6)**	93%		
(2) $R_1 = R_2 = R_3$ = Et	**(7)**	95%		
(3) $R_1 = R_2 = R_3$ = Ph	**(8)**	93%		
(4) $R_1 = R_2 = R_3$ = Cy	**(9)**	98%		
(5) $R_1 = R_2$ = Ph, $R_3 = CH_2PPh_2$	**(10)**	97%		
			(11)	93% 95%
			(12)	92% 94%
			(13)	93% 95%
			(14)	94% 95%
			(15)	95% 98%

Scheme 1. Synthesis of phosphine-stabilized 9-azido-9-borafluorenes (**6-10**) and bis(borafluorene-phosphinimine)s heterocycles (**11-15**). (Light source: broad spectrum from UV light, mercury vapor lamp. Details: ACE Glass 7825-34 Immersion UV lamp, 450 Watt, 5in Arc Length, Radial Lead, 6 FT Pin Cord.)

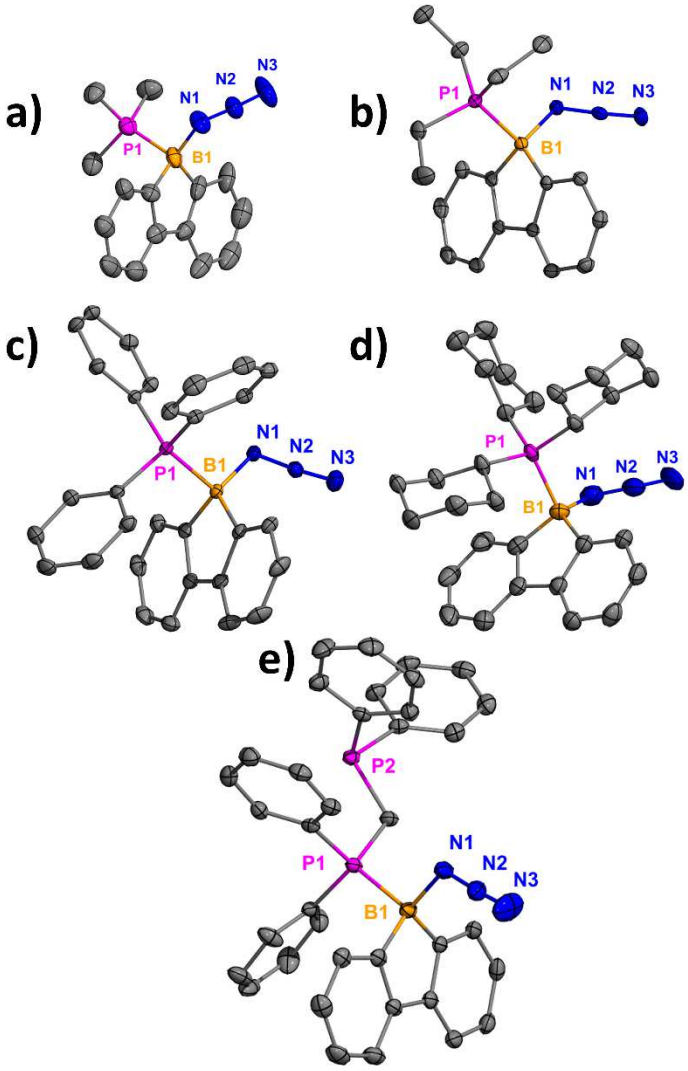

Figure 2. Molecular structures of **6** (a), **7** (b), **8** (c), **9** (d), and **10** (e). Thermal ellipsoids are set at 50% probability. H atoms were omitted for clarity, as was the co-crystallized solvent in **10**. Selected bond distances [Å]: **6**: B1–P1 1.9729(19), B1–N1 1.550(2); **7**: B1–P1 1.976(2), B1–N1

1.574(2); **8**: B1–P1 1.9971(13), B1–N1 1.5490(17); **9**: B1–P1 2.048(5), B1–N1 1.574(6); **10**: B1–P1 1.972(2), B1–N1 1.569(3).

Compounds **6-10** undergo thermolysis (120 °C) or photolysis in a pressure tube for 2 days to afford 4-membered B_2N_2 bis(borafluorene-phosphinimine)s **11-15** in 92-98% yields (Scheme 1). These reactions readily generate high yielding products due to complete conversion to BN spirocyclic compounds with dinitrogen (N_2) as the sole co-product. The $^{11}B\{^1H\}$ NMR chemical shifts of **11-15** range from -13.6 to 1.3 ppm. Compounds **11-15** were characterized by single crystal X-ray diffraction (Figure 3). The plane of the two borafluorene moieties in each structure is orthogonal to the 4-membered B_2N_2 ring. The spiro-boron atoms adopt a tetrahedral geometry in each structure. The P1-N1 bonds in **11-15** (1.5788(15)-1.591(2) Å) possess double bond character with bond distances similar to the P=N bonds in the phosphinimine compounds isolated by Stephan.[52, 54-56]

A PBE0-D3(BJ)/def2-SVP(CPCM, toluene) optimized geometry of **11** yields a P-N bond distance of 1.598 Å, consistent with the solid-state structure and similarly optimized examples of Stephan's phosphinimine compounds (1.583-1.607 Å).[52] The Mayer bond order is 1.45, indicative of P=N character (1.37-1.57 for Stephan's P=N compounds). It is noteworthy that Natural Bond Orbital (NBO) calculated Wiberg bond indices (WBI) underestimate the P-N bond order (1.02-1.05). Molecular orbital (MO) calculations of **11** and **13** yield a highest occupied MO (HOMO) with partial P-N π character that supports the assignment of a P=N bond (Figure 4). The LUMO in **11** is centered on the borafluorene π system while in **13** it is localized on the π system of the Ph groups in PPh_3.

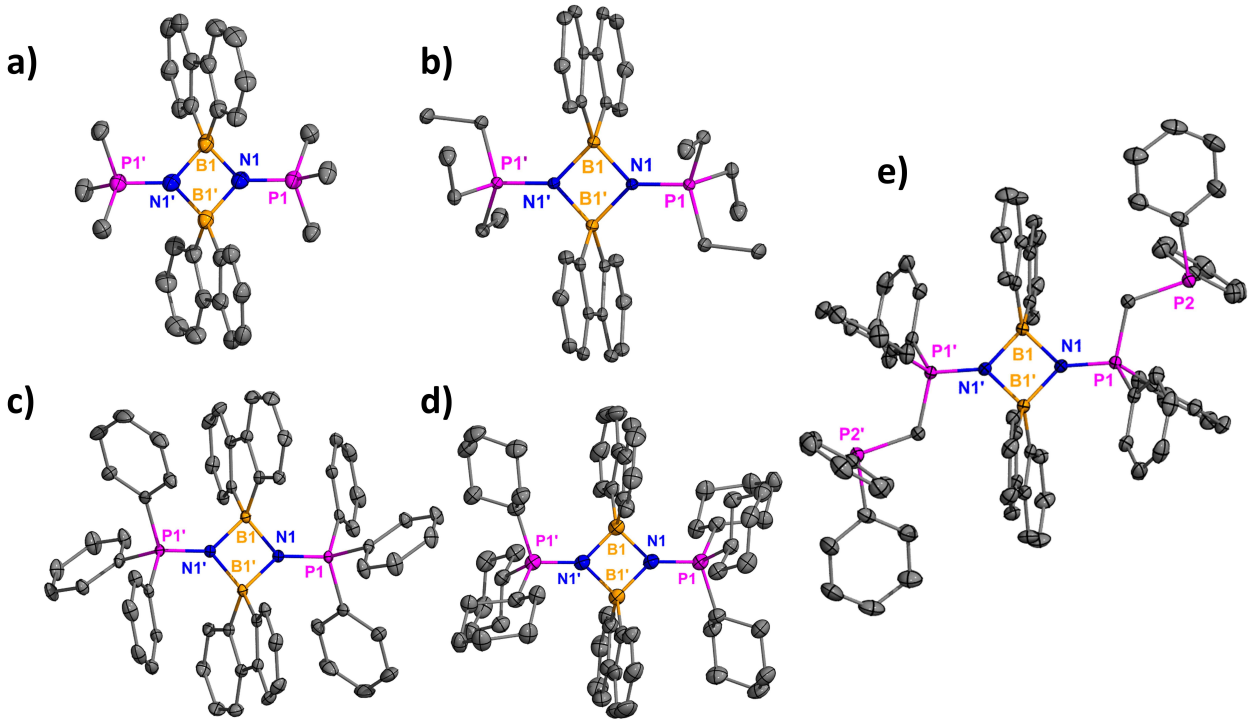

Figure 3. Molecular structures of **11** (a), **12** (b), **13** (c), **14** (d), and **15** (e). Thermal ellipsoids are set at 50% probability. H atoms were omitted for clarity, as was the disordered solvent in **11**. Selected bond distances [Å]**: 11**: B1–N1 1.550(5)**,** P1–N1 1.585(3); **12**: B1–N1 1.571(2), P1–N1 1.5806(14);**13**: B1–N1 1.5699(18), P1–N1 1.5804(11); **14**: B1–N1 1.582(4), P1–N1 1.591(2); **15**: B1–N1 1.573(2), P1–N1 1.5788(15).

The reactions to form **11-15** were hypothesized to proceed via intramolecular Staudinger-type mechanisms,[52, 57] which may be compared to work by Stephan on boron azides in intermolecular Staudinger oxidation reactions.[52, 55, 56] We also note that during the final preparation of this manuscript a preprint by Hoshimoto reported related reactions that also proceed via a Staudinger mechanism.[53]

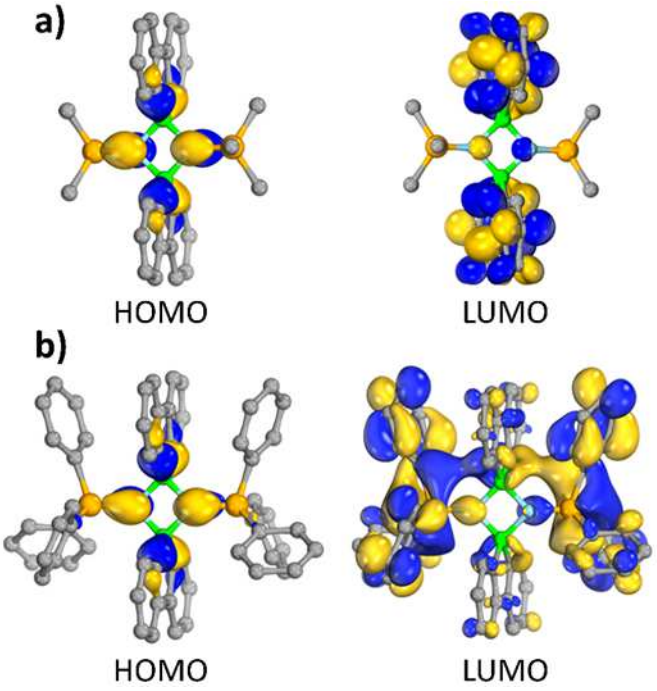

Figure 4. Plots of the HOMO and LUMO of (a) **11** (L = PMe_3) and (b) **13** (L = PPh_3) .

PBE0-D3(BJ)/def2-TZVPPD(CPCM,toluene)//PBE0-D3(BJ)/def2-SVP(CPCM,toluene).

A PBE0-D3(BJ)/def2-TZVPPD(CPCM,toluene)//PBE0-D3(BJ)/def2-SVP(CPCM, toluene) mechanistic study was carried out for the formation of **11**, with **6** (R = PMe_3) being considered representative of PR_3 systems. The calculated reaction energy pathway is illustrated in Figure 5. While not shown, initial addition of PMe_3 to 9-bromo-9-borafluorene (BF-Br) is favorable by 101.0 kJ mol^{-1} (ΔG) while subsequent replacement of Br by N_3 to form **6** is also favorable but by only 0.7 kJ mol^{-1}. The overall formation of **11** from **6** is very favorable, with ΔG of 285.1 kJ mol^{-1} (-386.1 kJ mol^{-1} if starting from 9-bromo-9-borafluorene).

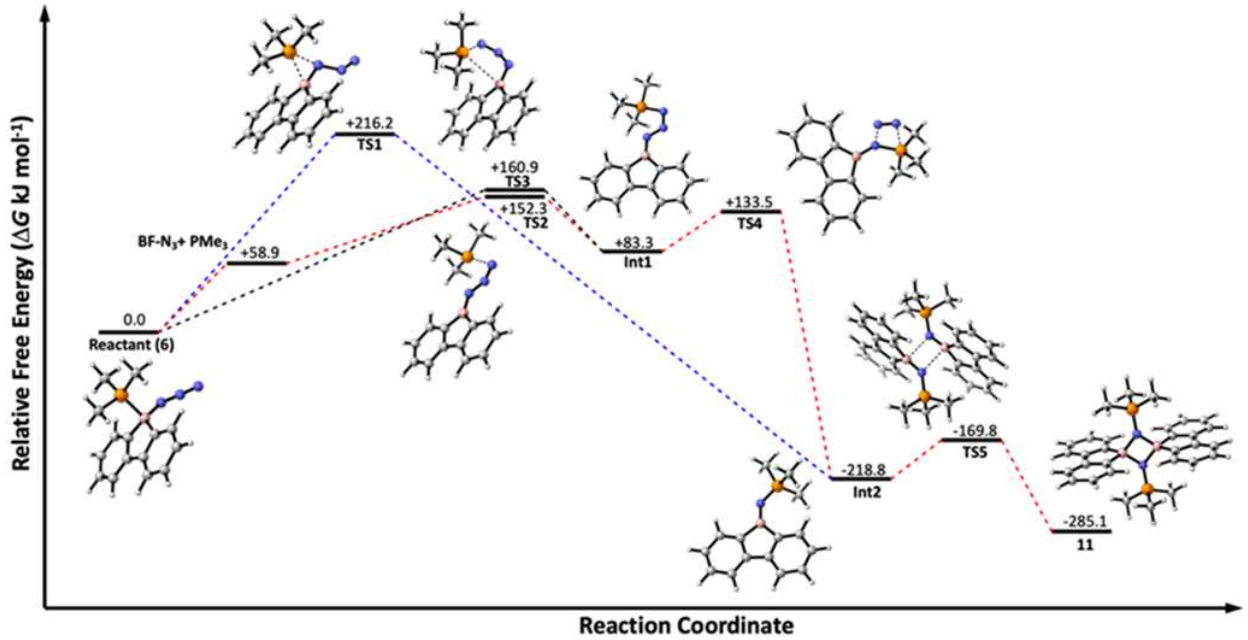

Figure 5. Calculated reaction pathway (ΔG, kJ mol^{-1}) for thermolysis reaction from **6** to **11**. PBE0-D3(BJ)/def2-TZVPPD(CPCM,toluene)//PBE0-D3(BJ)/def2-SVP(CPCM,toluene) results.

To explore the hypothesis of an intramolecular Staudinger-type mechanism from **6**, several pathways were considered. Migration of PMe_3 to either the α-nitrogen or γ-nitrogen of the azide could be considered as a first step toward the ejection of N_2. For α-N migration a transition state (**TS1**) was identified with a barrier of 216.2 kJ mol^{-1}, which is a very high barrier and unlikely to occur. Migration to γ-N has a smaller barrier of 160.9 kJ mol^{-1} (**TS3**) that leads to **Int1** (+83.3 kJ mol^{-1}) with PMe_3 bound to the terminal γ-N and the azide perpendicular to the borafluorene plane. Migration to γ-N is consistent with a Staudinger reaction. Alternatively, formation of **Int1** could occur in a two-step process with initial dissociation of PMe_3 from **6** (+58.9 kJ mol^{-1}) followed by addition of free PMe_3 to the γ-N of $BF\text{-}N_3$ (**TS2**, +152.3 kJ mol^{-1}). The formation of **Int1** could feasibly occur either by direct migration (**TS3**) or the two-step process (**TS2**) since the energetics are consistent with the forcing reaction conditions (120 °C or hν). For **Int1**, two conformations

were identified with the N_3P either co-planar with the borafluorene ring (energetically favored) or perpendicular to the borafluorene ring plane (0.4 kJ mol^{-1} higher in energy). The barrier between these conformers is only 9.3 kJ mol^{-1} (reverse barrier of 8.9 kJ mol^{-1}), suggesting that both conformations of **Int1** are accessible. The reaction energy profile in Figure 5 gives energies relative to the co-planar N_3P arrangement, however subsequent TSs to form **Int2** with either conformation have very similar barriers.

From **Int1**, a small barrier of 50.2 kJ mol^{-1} (**TS4**) associated with migration of PMe_3 from the γ-N to α-N and loss of N_2 leads to stable **Int2** (-218.8 kJ mol^{-1}). This is consistent with nucleophilic attack of the α-N to the phosphorus center. An unstable 4-membered N_3P ring intermediate might be expected from Staudinger reactivity, however no minima or TS associated with such a structure was located at this level of theory. Test calculations with a larger def2-TZVP basis set identified a minimum, although it is within 3 kJ mol^{-1} of **TS4** which suggests that a 4-membered N_3P ring complex is unstable or at most a shallow minimum on the reaction energy surface. Note that **Int2** is also directly linked with **TS1** (migration of PMe_3 from B to α-N), although with a much higher barrier. Finally, dimerization of **Int2** ([2+2] addition) has a small barrier of 48.9 kJ mol^{-1} (**TS5**) that yields the observed product **11** with a 4-coordinate boron. Here [2+2] addition is consistent with significant P=N character.

The phosphinimine or bora-iminophosphorane **Int2** could be considered an ylide B-N-P, ylene B-N=P, or ketene B=N=P. The Mayer bond order of P-N in **Int2** is 1.58, consistent with Stephan's phosphinimine compounds (1.37-1.57), while the B-N bond order is 1.34. For reference, the two B-C bonds have bond orders of 0.90 and 1.01. The B-N-P bond angle is 134.8°, which leaves the B atom sterically accessible for nucleophilic attack. Both B-N and P-N bonds in **Int2** have significant double bond character, with the dominant resonance structures being the ylene (B-N=P)

and ketene (B=N=P) forms. It is noteworthy that the phosphorus center is oxidized from III to V and it goes from being involved in only σ-bonding with the boron center to including partial σ and π bonding with the nitrogen atom.

The formation of **Int1** (PMe_3 migration to γ-N) is the rate determining step. The calculated reaction pathway is consistent with a Staudinger-type reaction for the formation of **11**; formation of compound **11-15** likely involves an iminophosphorane intermediate (**Int2**) via release of dinitrogen (N_2). To the best of our knowledge, these are the first examples of *intra*molecular Staudinger-type reactions, which involve Lewis base migration from boron.

To study the photophysical properties of spirocyclic compounds **11-15**, UV-Vis and fluorescence spectroscopy, absolute quantum yield measurements, and fluorescence lifetime studies were carried out (Table 1 and Figure 6). In toluene, compounds **11-15** show UV-Vis absorption bands in the 291-340 nm range, and emission bands ~350 nm. However, compounds **11**, **12**, and **15** show a second emission band at ~530 nm. The first emission band corresponds to the transition from the first excited state to the ground state whereas the second emission band is a result of an intramolecular charge transfer (ICT) from ligands to heterocycles. Also, the PL lifetime measurements supports the origin of the intramolecular charge transfer band, which display biexponential decay for compounds **11-15** (Table 1). The τ_{s1} is the lifetime for lower emission bands and τ_{s2} is for the ICT bands. In efforts to quantify the luminescence of **11-15**, absolute quantum yields (Φ_F) were determined in toluene (Table 1). Compound **12** had the lowest quantum yield of Φ_F = 13% and compound **14** had the highest absolute quantum yield with Φ_F = 68%.

Table 1. Photophysical data of 4-membered B-N spirocyclic compounds **12-15** in toluene.

Compounds	λ_{abs} (nm)	λ_{em} (nm)	$\Phi_F^{[solution]}$ (%)	$\Phi_F^{[solid]}$ (%)	τ_s1 (ns)	τ_s2 (ns)
11	282,306	375, 525	37	12	3.40 (64%)	16.07 (36%)
12	306, 320	345, 525	13	9	0.17 (24%)	3.77 (76%)
13	295,342	350	61	10	0.49 (60%)	7.09 (40%)
14	291,306	350	68	11	0.17 (64%)	2.14 (36%)
15	306, 320	350,525	17	13	0.10 (51%)	3.13 (49%)

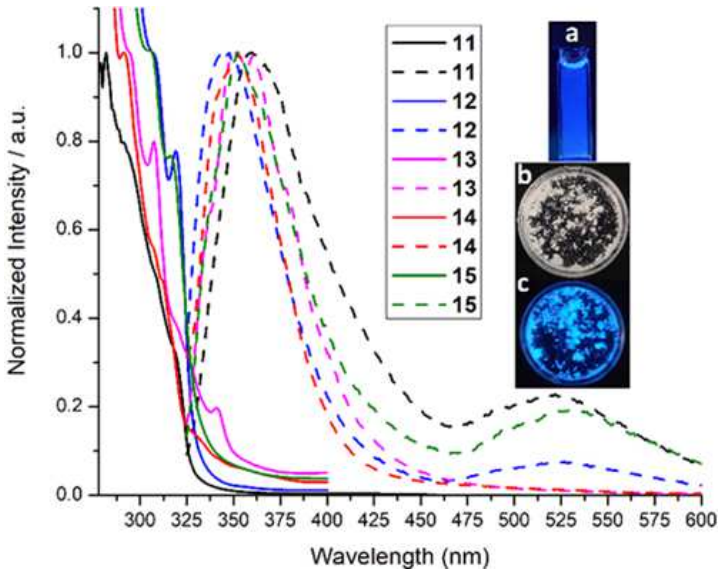

Figure 6. Normalized absorption (solid line) and emission (dashed line) spectra of **11** (black), **12** (blue), **13** (pink), **14** (red), and **15** (green) in toluene. All compounds were excited at 320 nm. Images a, b, and c represent solution fluorescence under UV-light (λ = 355 nm), solid under ambient light, and solid-state fluorescence under UV-light (λ = 355 nm), respectively for compounds **11-15**.

Conclusion

We have reported a new BN-containing heterocycles formed via intramolecular Staudinger-type reactions which contain bis(borafluorene-phosphinimine) moieties. The key reaction steps involve light- or heat-initiated release of dinitrogen, migration of the phosphine from boron to nitrogen, and oxidation of the phosphorus center (III to V). Theoretical calculations are consistent with a Staudinger-type mechanisms, with migration of phosphine to nitrogen being the rate determining. The 4-membered B_2N_2-spirocyclic borafluorene compounds exhibit blue fluorescence in the solution and solid states with absolute quantum yields (Φ_F) up to 68%. These studies contribute to the goal within the main-group synthetic community aimed at the discovery of new boron heterocycles with interesting reactivity trends, electronic structures, and optical properties.

Experimental Section

General Procedures: All air- and moisture-sensitive reactions were performed under an inert atmosphere of argon using standard Schlenk techniques or in a MBRAUN LABmaster glovebox equipped with a -37 °C freezer. Reaction solvents including toluene and hexanes were purified by distillation over sodium, while ethereal solvents such as diethyl ether and tetrahydrofuran (THF) were purified by distillation over Na/benzophenone. Dichloromethane (DCM) was purified via distillation over calcium hydride (CaH_2). Deuterated solvents were purchased from Acros Organics and Cambridge Isotope Laboratories and dried over sodium (C_6D_6) and Na/K alloy (THF- d_8). All glassware used for reactions was oven-dried at 190 °C overnight. The NMR spectra were recorded at 298.15 K on a Varian 600 MHz spectrometer. Proton and carbon chemical shifts are reported in ppm and are referenced using the residual proton and carbon signals of the deuterated solvent (^{1}H: C_6D_6 δ= 7.16, THF-d_8 δ= 3.58, 1.72; ^{13}C: C_6D_6 δ= 128.06, THF-d_8 δ= 67.21, 25.31). All boron signals are reported in ppm and were referenced to an external standard, $BF_3{\cdot}Et_2O$ (^{11}B: δ = 0.00). Due to a borosilicate NMR probe, there is a broad signal observed from -25 to 25 ppm. ^{31}P NMR chemical shifts were referenced to an 85% phosphoric acid standard (^{31}P: δ = 0.00). Solid-state FTIR spectra were recorded in an argon-filled glovebox on an Agilent Cary 630 FT-IR equipped with a diamond ATR unit. Single crystal X-ray diffraction data collection and structure refinement details are given in the X-ray crystallographic section of the SI. Elemental analyses were performed using a Perkin-Elmer 2400 Series II analyzer. The following compounds were prepared according to literature procedures: 9-halo-9-borafluorene,[39, 47] and 9-azido-9-borafluorene.[47, 48, 58] All other compounds were purchased from Sigma-Aldrich and Fisher Scientific and used without further purification.

UV-vis/ Fluorescence

UV-vis data were collected on a Cary 60 UV-vis spectrometer. Fluorescence data were collected on a Cary Eclipse fluorescence spectrometer. Samples were dissolved in toluene, and data were collected in 1 cm square quartz cuvettes.

Quantum Yields

Absolute fluorescence quantum yields were determined using a Hamamatsu C11347-11 Quantaurus-QY Absolute PL Quantum Yield Spectrometer. Samples were prepared inside the glovebox 1 cm square quartz cuvettes (solutions). Solutions were prepared in THF, and data were collected with absorbance values below 0.1.

Fluorescence Lifetime

Lifetime data were collected using Edinburgh Instruments Spectrofluorometer FS5. Samples were prepared inside the glovebox using 1 cm square quartz cuvettes (solutions). Solutions were prepared in toluene and data were collected with absorbance values below 0.1. A Ludox® (colloidal silica) solution was used to measure the instrument response function (IRF). Lifetime fitting was completed using the Fluorophore software and χ^2 values between 0.8 and 1.5 with the smallest number of components being used as the best fit.

CAUTION: *Boron azides described here may be shock-sensitive and/or explosive. They need to be handled under an inert atmosphere for appropriate safety precautions.*

General procedure for preparation of phosphine-stabilized 9-bromo-9-borafluorene adducts (1-5)

To a solution of 9-bromo-9-borafluorene **(BF-Br)** (1.0 equiv) in toluene, the corresponding phosphine ligand **L** (1.0 equiv) was added. The resulting mixture was allowed to stir for 4 hours. All volatile components were removed in vacuo and the remaining solid was washed with 10 mL of hexanes/toluene (1:1) mixture and dried to leave the product as a white solid, **R_3P-BF-Br**.

Me_3P-BF-Br. Compound **1** was prepared according to the general procedure using trimethyl phosphine (Me_3P) (1.24 mmol, 0.943 g) and 9-bromo-9-borafluorene (1.24 mmol, 0.300 g) in 95% yield (0.344 g) as a white solid. **^{1}H NMR** (600 MHz, C_6D_6) δ 7.66 (d, J = 9 Hz, 2H, BF-ArH), 7.64 (d, J = 7 Hz, 2H, BF-ArH), 7.27 (t, J = 8 Hz, 2H, BF-ArH), 7.21 (t, J = 7 Hz, 2H, BF-ArH), 0.46 (d, J = 11 Hz, 9H, CH_3 in Me_3P). **^{13}C NMR** (151 MHz, C_6D_6) δ 131.46 (ArC), 128.35 (ArC), 126.98 (ArC), 120.13 (ArC), 6.28 (CH_3 in Me_3P). **^{11}B{^{1}H} NMR** (192 MHz, C_6D_6) δ -5.7 ppm. **^{31}P{^{1}H} NMR** (243 MHz, C_6D_6) δ -12.67 ppm. Anal. Calcd. For $C_{15}H_{17}BBrP$: C, 56.48; H, 5.37 %. Found C, 56.80; H, 5.65 %. Note: Some of the C peaks were not discernable in the ^{13}C NMR spectrum due to the limited solubility of compound 1 in C_6D_6.

Et_3P-BF-Br. Compound **2** was prepared according to the general procedure using triethyl phosphine (Et_3P) (3.44 mmol, 0.410 g, 0.500 mL) and 9-bromo-9-borafluorene (0.820 mmol, 0.200 g) in 96% yield (0.297 g) as a white solid**. ^{1}H NMR** (600 MHz, C_6D_6) δ 7.73 (t, *J* = 7 Hz, 2H, BF-Ar*H*), 7.66 (t, *J* = 5 Hz, 2H, BF-Ar*H*), 7.26 (d, *J* = 6 Hz, 2H, BF-Ar*H*), 7.22 (d, *J* = 6 Hz, 2H, BF-Ar*H*), 1.19 (m, 6H, C*H*$_2$ in Et_3P), 0.49 – 0.42 (m, 9H, , C*H*$_3$ in Et_3P) ppm. **^{13}C NMR** (151 MHz, C_6D_6) δ 151.26 (Ar*C*), 148.97 (Ar*C*) 132.03 (Ar*C*), 128.40 (Ar*C*), 126.95 (Ar*C*), 120.16 (Ar*C*), 11.74 (*C*H_2 in Et_3P) 6.77 (*C*H_3 in Et_3P) ppm. **^{11}B{^{1}H} NMR** (192 MHz, C_6D_6) δ -9.6 ppm. **^{31}P{^{1}H}**

NMR (243 MHz, C_6D_6) δ -0.33 ppm. Anal. Calcd. For $C_{18}H_{23}BBrP$: C, 59.88; H, 6.42 %. Found C, 59.83; H, 6.51 %.

Ph_3P-BF-Br. Compound **3** was prepared according to the general procedure using triphenyl phosphine (Ph_3P) (0.650 mmol, 0.171 g) and 9-bromo-9-borafluorene (0.540 mmol, 0.170 g) in 92% yield (0.251 g) as a white solid. **^{1}H NMR** (600 MHz, C_6D_6) δ 7.79 – 7.74 (m, 2H, BF-Ar*H*), 7.64 (t, *J* = 9 Hz, 6H, Ar*H* in PPh_3), 7.45 (d, *J* = 9 Hz, 2H, BF-Ar*H*), 7.12 (tt, *J* = 8, 1 Hz, 2H, BF-Ar*H*), 7.04 (dd, *J* = 7, 1 Hz, 2H, BF-Ar*H*), 6.92 (t, *J* = 8 Hz, 3H, Ar*H* in PPh_3), 6.87 – 6.82 (m, 6H, Ar*H* in PPh_3) ppm. **^{13}C NMR** (151 MHz, C_6D_6) δ 149.55 (Ar*C)*, 134.50 (Ar*C)*, 132.95 (Ar*C)*, 131.74 (Ar*C)*, 128.66 (Ar*C)*, 128.59 (Ar*C)*, 126.89 (Ar*C)*, 126.39 (Ar*C)*, 126.01 (Ar*C)*, 119.82 (Ar*C)* ppm. **^{11}B{^{1}H} NMR** (192 MHz, C_6D_6) δ -7.3 ppm. **^{31}P{^{1}H} NMR** (243 MHz, C_6D_6) δ 1.75 ppm. Data reported in $CDCl_3$ by Rivard.[35]

Cy_3P-BF-Br. Compound **4** was prepared according to the general procedure using tricyclohexyl phosphine (Cy_3P) (0.996 mmol, 0.280 g) and 9-bromo-9-borafluorene (0.996 mmol, 0.242 g) in 87% yield (0.453 g) as a white solid. **^{1}H NMR** (600 MHz, THF-d_8) δ 7.61 (d, *J* = 8 Hz, 2H, BF-Ar*H*), 7.57 (d, *J* = 7 Hz, 2H, BF-Ar*H*), 7.18 (t, *J* = 7 Hz, 2H, BF-Ar*H*), 7.09 (t, *J* = 8 Hz, 2H, BF-Ar*H*), 2.38 – 2.31 (m, 3H, PCy_3–*H*), 2.11 (s, 6H, PCy_3–*H*,), 1.65 (d, *J* = 13 Hz, 6H, PCy_3–*H*), 1.24 (m, 15H, PCy_3–*H*), 1.12 (d, *J* = 13 Hz, 3H, PCy_3–*H*). **^{13}C NMR** (151 MHz, THF-d_8) δ 133.49 (Ar*C)*, 129.85 (Ar*C)*, 129.09 (Ar*C)*, 128.30 (Ar*C)*, 127.10 (Ar*C)*, 120.30 (Ar*C)*, 33.23 (PCy_3–*C*), 29.81 (PCy_3–*C*), 28.37 (PCy_3–*C*), 27.68 (PCy_3–*C*). **^{11}B{^{1}H} NMR** (192 MHz, THF-d_8) δ -8.1 ppm. **^{31}P{^{1}H} NMR** (243 MHz, THF-d_8) δ -1.78 ppm. Data reported in $CDCl_3$ by Rivard.[35]

$Ph_2PCH_2(Ph_2)$P-BF-Br. Compound **5** was prepared according to the general procedure using bis(diphenylphoshpino)methane ($Ph_2PCH_2(Ph_2)$P) (1.16 mmol, 0.447 g) and 9-bromo-9-borafluorene (1.16 mmol, 0.282 g) in 95% yield (0.693 g) as a white solid. **^{1}H NMR** (600 MHz, THF-d_8) δ 7.41 (d, *J* = 11 Hz, 2H, BF-Ar*H*), 7.37 – 7.30 (m, 8H, Ar*H*), 7.25 – 7.19 (m, 12H, Ar*H*), 7.12 (d, *J* = 6 Hz, 2H, BF-Ar*H*), 7.06 (d, *J* = 4 Hz, 2H, BF-Ar*H*), 7.02 – 6.90 (m, 2H, BF-Ar*H*), 3.44 (s, 2H, P-C*H*-P) ppm. **^{13}C NMR** (151 MHz, THF-d_8) δ 149.78 (Ar*C*), 134.98 (Ar*C*), 133.73 (Ar*C*), 133.59 (Ar*C*), 132.81 (Ar*C*), 132.60 (Ar*C*), 129.94 (Ar*C*), 129.50 (Ar*C*), 129.20 (Ar*C*), 128.88 (Ar*C*), 128.45 (Ar*C*), 127.05 (Ar*C*), 120.09 (Ar*C*), 20.61 (P-*C*H-P) ppm. **^{11}B{^{1}H} NMR** (192 MHz, THF-d_8) δ -7.6 ppm. **^{31}P{^{1}H} NMR** (243 MHz, THF-d_8) δ 3.08, -20.44 ppm. Anal. Calcd. For $C_{37}H_{30}BBrP_2$: C, 70.84; H, 4.82 %. Found C, 71.07; H, 5.01 %.

General procedure for preparation of phosphine-stabilized 9-azido-9-borafluorene adducts (6-10)

To a solution of phosphine-stabilized 9-bromo-9-borafluorene (**1-5**), in toluene (1.0 equiv), excess trimethylsilyl azide was added. The reaction mixture was stirred for 4 hours. All volatile components were removed *in vacuo* and the residue was washed with 10 mL of hexanes and dried under vacuum to afford the product as a white solid, **R_3P-BF-N_3**.

Me_3P-BF-N_3. Compound **6** was synthesized according to the general procedure by a reaction between compound **1** (0.313 mmol, 0.100 g) and trimethylsilyl azide (0.942 mmol, 0.111 g, 0.200 mL) in 93% yield (0.0818 g) as a white solid. **^{1}H NMR** (600 MHz, C_6D_6) δ 7.70 (d, *J* = 8 Hz, 2H, BF-Ar*H*), 7.60 (d, *J* = 8 Hz, 2H, BF-Ar*H*), 7.30 (t, *J* = 2 Hz, 2H, BF-Ar*H*), 7.22 (m, 2H, BF-Ar*H*), 0.31 (d, *J* = 11 Hz, 9H, C*H*$_3$ in Me_3P) ppm. **^{13}C NMR** (151 MHz, C_6D_6) δ 149.12 (Ar*C*), 130.78 (Ar*C*), 129.34 (Ar*C*), 128.35 (Ar*C*), 126.81 (Ar*C*), 120.25 (Ar*C*), 6.07 (*C*H$_3$ in Me_3P) ppm.

$^{11}B\{^1H\}$ NMR (192 MHz, C_6D_6) δ -7.1 ppm. **$^{31}P\{^1H\}$ NMR** (243 MHz, C_6D_6) δ -12.16 ppm. Anal. Calcd. For $C_{15}H_{17}BN_3P$: C, 64.09; H, 6.10; N, 14.95 %. Found C, 64.10; H, 6.45; N, 14.70 %.

Et_3P-BF-N_3. Compound **7** was synthesized according to the general procedure by a reaction between compound **2** (0.277 mmol, 0.100 g) and trimethylsilyl azide (1.39 mmol, 0.160 g, 0.2 mL) in 95% yield (0.0850 g) as a white solid. **^1H NMR** (600 MHz, C_6D_6) δ 7.69 (d, *J* = 8 Hz, 2H, BF-Ar*H*), 7.65 (d, *J* = 9 Hz, 2H, BF-Ar*H*), 7.33 – 7.27 (m, 2H, BF-Ar*H*), 7.26 – 7.22 (m, 2H, BF-Ar*H*), 1.04 – 0.96 (m, 6H, C*H*$_2$ in Et_3P), 0.48 – 0.41 (m, 9H, C*H*$_3$ in Et_3P) ppm. **^{13}C NMR** (151 MHz, C_6D_6) δ 149.19 (Ar*C*), 131.14 (Ar*C*), 130.71 (Ar*C*), 129.16 (Ar*C*), 126.77 (Ar*C*), 120.27 (Ar*C*), 11.03 (*C*H$_2$ in Et_3P), 6.33 (*C*H$_3$ in Et_3P) ppm. **$^{11}B\{^1H\}$ NMR** (192 MHz, C_6D_6) δ -5.9 ppm. **$^{31}P\{^1H\}$ NMR** (243 MHz, C_6D_6) δ 1.93 ppm. Anal. Calcd. For $C_{18}H_{23}BN_3P$: C, 66.90; H, 7.17; N, 13.00 %. Found C, 66.79; H, 7.15; N, 13.35 %.

Ph_3P-BF-N_3. Compound **8** was synthesized according to the general procedure by a reaction between compound **3** (0.200 mmol, 0.100 g) and trimethylsilyl azide (7.55 mmol, 1.00 mL) in 93% yield (0.0870 g) as a white solid. **^1H NMR** (600 MHz, C_6D_6) δ 7.68 (d, *J* = 9 Hz, 2H, BF-Ar*H*), 7.49 – 7.41 (m, 8H, BF-Ar*H* and ArH in PPh_3), 7.15 – 7.13 (m, 2H, BF-Ar*H*), 7.03 (t, *J* = 7 Hz, 2H, BF-Ar*H*), 6.95 – 6.91 (m, 3H, Ar*H* in PPh_3), 6.90 – 6.85 (m, 6H, Ar*H* in PPh_3) ppm. **^{13}C NMR** (151 MHz, C_6D_6) δ 150.08 (Ar*C)*, 133.97 (Ar*C)*, 132.20 (Ar*C)*, 131.32 (Ar*C)*, 128.83 (Ar*C)*, 128.76 (Ar*C)*, 126.76 (Ar*C)*, 119.92 (Ar*C)* ppm. **$^{11}B\{^1H\}$ NMR** (192 MHz, C_6D_6) δ 1.7 ppm. **$^{31}P\{^1H\}$ NMR** (243 MHz, C_6D_6) δ 2.00 ppm. Anal. Calcd. For $C_{30}H_{23}BN_3P$: C, 77.11; H, 4.96; N, 8.99 %. Found C, 77.49; H, 4.85; N, 8.74 %.

Cy_3P-BF-N_3. Compound **9** was synthesized according to the general procedure by a reaction between compound **4** (0.287 mmol, 0.150 g) and trimethylsilyl azide (2.87 mmol, 0.400 mL) in 98% yield (0.136 g) as a white solid. **^{1}H NMR** (600 MHz, C_6D_6) δ 7.81 (d, *J* = 7 Hz, 2H, BF-Ar*H*), 7.70 (d, *J* = 6 Hz, 2H, BF-Ar*H*), 7.33 – 7.23 (m, 4H, BF-Ar*H*), 2.05 (q, *J* = 12 Hz, 3H, PCy_3–*H*), 1.82 (d, *J* = 13 Hz, 6H, PCy_3–*H*), 1.52 (d, *J* = 11 Hz, 6H, PCy_3–*H*), 1.43 (d, *J* = 9 Hz, 3H, PCy_3–*H*), 1.07 – 0.91 (m, 15H, PCy_3–*H*). **^{13}C NMR** (151 MHz, C_6D_6) δ 149.69 (Ar*C*), 131.85 (Ar*C*), 129.31 (Ar*C*), 128.35 (Ar*C*), 126.86 (Ar*C*), 120.35 (Ar*C*), 31.94 (PCy_3–*C*), 31.79 (PCy_3–*C*), 28.34 (PCy_3–*C*), 28.32 (PCy_3–*C*), 27.75 (PCy_3–*C*), 27.68 (PCy_3–*C*), 26.29 (PCy_3–*C*) ppm.**^{11}B{^{1}H} NMR** (192 MHz, C_6D_6) δ -5.7 ppm. **^{31}P{^{1}H} NMR** (243 MHz, C_6D_6) δ 0.78 ppm. Anal. Calcd. For $C_{30}H_{41}BN_3P$: C, 74.22; H, 8.51; N, 8.66 %. Found C, 73.96; H, 8.47; N, 8.50 %.

$Ph_2PCH_2(Ph_2)P$-BF-N_3. Compound **10** was synthesized according to the general procedure by a reaction between compound **5** (0.247 mmol, 0.155 g) and trimethylsilyl azide (2.47 mmol, 0.300 mL) in 97% yield (0.141 g) as a white solid. **^{1}H NMR** (600 MHz, C_6D_6) δ 7.77 (d, *J* = 7 Hz, 2H, BF-Ar*H*), 7.40 (d, *J* = 7 Hz, 2H, BF-Ar*H*), 7.24 – 7.18 (m, 8H, Ar*H*), 7.15 – 7.12 (m, 2H, BF-Ar*H*), 7.11 – 7.06 (m, 3H, Ar*H*), 7.07 – 6.99 (m, 2H, BF-Ar*H*), 6.92 – 6.87 (m, 4H, Ar*H*), 6.82 (t, *J* = 5 Hz, 8H, Ar*H*), 3.17 (s, 2H, P-C*H*-P). **^{13}C NMR** (151 MHz, C_6D_6) δ 149.59 (Ar*C*), 133.37 (Ar*C*), 133.27 (Ar*C*), 131.75 (Ar*C*), 130.32 (Ar*C*), 129.33 (Ar*C*), 128.61 (Ar*C*), 128.55 (Ar*C*), 126.70 (Ar*C*), 125.69 (Ar*C*), 120.00 (Ar*C*), 20.76 (P-*C*H-P) ppm. **^{11}B{^{1}H} NMR** (192 MHz, C_6D_6) δ -2.9 ppm. **^{31}P{^{1}H} NMR** (243 MHz, C_6D_6) δ 8.13, -29.49 ppm. Anal. Calcd. For $C_{37}H_{30}BN_3P_2$: C, 75.40; H, 5.13; N, 7.13 %. Found C, 75.02; H, 5.33; N, 7.33 %.

General procedure for the preparation of the 4-membered BN spirocyclic compound (11-15)

Thermolysis: A solution of phosphine-stabilized 9-azido-9-borafluorene in C_6D_6 solvent was refluxed for two days in a J-young tube. The solution changed from colorless to light yellow color. The reaction was tracked using $^{11}B\{^1H\}$ and $^{31}P\{^1H\}$ NMR that confirmed complete conversion to the desired product after two days. C_6D_6 solvent was removed in vacuo, and the remaining solid was redissolved in DCM, then concentrated for recrystallization at -37 °C temperature.

Photolysis: A solution of phosphine-stabilized 9-azido-9-borafluorene in C_6D_6 solvent was exposed to light using a photoreactor for two days in a J-young. The solution changed from colorless to brown. The reaction was tracked using $^{11}B\{^1H\}$ and $^{31}P\{^1H\}$ NMR that confirmed complete conversion to the desired product after two days. C_6D_6 solvent was removed in vacuo, and the remaining solid was redissolved in DCM, then concentrated for recrystallization at -37 °C temperature.

Light Source: The photolysis was performed using ACE Glass INC 7825-34 Immersion UV Lamp, 450 Watt, 5in ARC Length, Radial Lead, 6 FT Pin Cord.

(Me_3P=N-BF)$_2$. Compound **11** was prepared according to the general procedures using trimethylphosphine-stabilized 9-azido-9-borafluorene **6** (0.178 mmol, 50 mg). **Thermolysis** (93% yield, 41.9 mg); **Photolysis** (95% yield, 42.7 mg). **^{1}H NMR** (600 MHz, C_6D_6) δ 8.41 (d, *J* = 5 Hz, 4H, BF-Ar*H*), 7.85 (d, *J* = 8 Hz, 4H, BF-Ar*H*), 7.50 – 7.45 (m, 4H, BF-Ar*H*), 7.43 – 7.39 (m, 4H, BF-Ar*H*), 0.36 (m, 18H, C*H*$_3$ in Me_3P). **^{13}C NMR** (151 MHz, C_6D_6) δ 148.66 (Ar*C*), 131.28 (Ar*C*), 129.54 (Ar*C*), 127.27 (Ar*C*), 126.89 (Ar*C*), 119.19 (Ar*C*), 14.56 (*C*H$_3$ in Me_3P). **^{11}B{^{1}H} NMR** (192 MHz, C_6D_6) δ -13.6 ppm. **^{31}P{^{1}H} NMR** (243 MHz, C_6D_6) δ 31.72 ppm.

(Et_3P=N-BF)$_2$. Compound **12** was prepared according to the general procedure using triethylphosphine-stabilized 9-azido-9-borafluorene **7** (0.154 mmol, 50.0 mg). **Thermolysis** (92% yield, 42.0 mg); **Photolysis** (94% yield, 43.4 mg). **^{1}H NMR** (600 MHz, C_6D_6) δ 8.52 (d, *J* = 7 Hz, 2H, BF-Ar*H*), 7.84 (d, *J* = 7 Hz, 2H, BF-Ar*H*), 7.49 (td, *J* = 7, 1 Hz, 2H, BF-Ar*H*), 7.40 (td, *J* = 7, 1 Hz, 2H, BF-Ar*H*), 0.89 (m, 6H, C*H*$_2$ in Et_3P), 0.34 (m, 9H, C*H*$_3$ in Et_3P). **^{13}C NMR** (151 MHz, C_6D_6) δ 131.14 (Ar*C*), 128.33 (Ar*C*), 126.77 (Ar*C*), 120.27 (Ar*C*), 14.00 (*C*H$_2$ in Et_3P), 7.00(*C*H$_3$ in Et_3P) ppm. **^{11}B{^{1}H} NMR** (192 MHz, C_6D_6) δ 1.3 ppm. **^{31}P{^{1}H} NMR** (243 MHz, C_6D_6) δ 38.50 ppm. For $C_{36}H_{46}B_2N_2P_2$: C, 73.24; H, 7.85; N, 4.75 %. Found C, 73.55; H, 7.90; N, 4.47 %.

(Ph_3P=N-BF)$_2$. Compound **13** was prepared according to the general procedure using triphenylphosphine-stabilized 9-azido-9-borafluorene **8** (0.0500 mmol, 30.0 mg). **Thermolysis** (93% yield, 26.5 mg); **Photolysis** (95% yield, 27 mg). **^{1}H NMR** (600 MHz, C_6D_6) δ 7.76 – 7.72 (m, 10H, Ar*H* in PPh_3), 7.56 (d, *J* = 8 Hz, 4H, BF-Ar*H*), 7.44 (d, *J* = 9 Hz, 4H, BF-Ar*H*), 7.22 (d, *J* = 8 Hz, 4H, BF-Ar*H*), 7.09 – 7.02 (m, 12H, BF-Ar*H* and Ar*H* in PPh_3), 6.98 – 6.94 (m, 12H, Ar*H* in PPh_3) ppm. **^{13}C NMR** (151 MHz, C_6D_6) δ 153.26 (Ar*C)*, 134.28 (Ar*C)*, 134.15 (Ar*C)*, 133.57 (Ar*C)*, 132.73 (Ar*C)*, 132.67 (Ar*C)*, 131.83 (Ar*C)*, 131.05 (Ar*C)*, 128.82 (Ar*C)*, 128.74 (Ar*C)*, 127.55 (Ar*C)*, 119.58 (Ar*C)* ppm. **^{11}B{^{1}H} NMR** (192 MHz, C_6D_6) δ -5.8 ppm. **^{31}P{^{1}H} NMR** (243 MHz, C_6D_6) δ 7.16 ppm. For $C_{60}H_{46}B_2N_2P_2$: C, 82.02; H, 5.28; N, 3.19 %. Found C, 81.90; H, 5.60; N, 3.43 %.

(Cy_3P=N-BF)$_2$. Compound **14** was prepared according to the general procedure using tricyclohexylphosphine-stabilized 9-azido-9-borafluorene **9** (0.0800 mmol, 40.0 mg). **Thermolysis** (94% yield, 34.4 mg); **Photolysis** (95% yield, 34.8 mg). **^{1}H NMR** (600 MHz, C_6D_6) δ 7.89 – 7.85 (m, 4H, BF-Ar*H*), 7.64 – 7.59 (m, 4H, BF-Ar*H*), 7.33 – 7.29 (m, 8H, BF-Ar*H*), 1.90

(s, 14H, PCy_3–*H*), 1.73 (d, *J* = 13 Hz, 4H, PCy_3–*H*), 1.64 (s, 10H, PCy_3–*H*), 1.54 (d, *J* = 11 Hz, 6H, PCy_3–*H*), 1.39 (d, *J* = 11 Hz, 16H, PCy_3–*H*), 1.06 (d, *J* = 11 Hz, 16H, PCy_3–*H*). **^{13}C NMR** (151 MHz, C_6D_6) δ 152.96 (Ar*C)*, 130.68 (Ar*C)*, 130.62 (Ar*C)*, 129.33 (Ar*C)*, 127.44 (Ar*C)*, 119.66 (Ar*C)*, 36.55 (PCy_3–*C*), 36.14 (PCy_3–*C*), 32.34 (PCy_3–*C*), 32.21 (PCy_3–*C*), 31.75 (PCy_3–*C*), 31.67 (PCy_3–*C*), 28.53 (PCy_3–*C*), 28.09 (PCy_3–*C*), 28.03 (PCy_3–*C*), 27.49 (PCy_3–*C*), 26.99 (PCy_3–*C*), 26.42 (PCy_3–*C*), 23.06 (PCy_3–*C*), 14.35 (PCy_3–*C*). **^{11}B{^{1}H} NMR** (192 MHz, C_6D_6) δ -2.3 ppm. **^{31}P{^{1}H} NMR** (243 MHz, C_6D_6) δ 9.82 ppm. For $C_{60}H_{82}B_2N_2P_2$: C, 78.77; H, 9.03; N, 3.06 %. Found C, 78.56; H, 8.70; N, 3.21 %.

($Ph_2PCH_2(Ph_2)P$=N-BF)$_2$. Compound **15** was prepared according to the general procedure using bis(diphenylphosphino)methane-stabilized 9-azido-9-borafluorene (0.0500 mmol, 35.0 mg). **Thermolysis** (95% yield, 26.7 mg); **Photolysis** (98% yield, 27.6 mg). **^{1}H NMR** (600 MHz, C_6D_6) δ 7.78 (d, *J* = 7 Hz, 4H, BF-Ar*H*), 7.40 (d, *J* = 7 Hz, 4H, BF-Ar*H*), 7.28 (t, *J* = 8 Hz, 16H, Ar*H* in $CH_2(PPh2)_2$), 7.15 – 7.11 (m, 4H, BF-Ar*H*), 7.08 (t, *J* = 8 Hz, 4H, BF-Ar*H*), 7.06 – 7.00 (m, 4H, Ar*H* in $CH_2(PPh2)_2$), 6.94 (t, *J* = 8 Hz, 8H, Ar*H* in $CH_2(PPh2)_2$), 6.90 – 6.87 (m, 12H, Ar*H* in $CH_2(PPh2)_2$), 3.05 (s, 4H, CH_2). **^{11}B{^{1}H} NMR** (192 MHz, C_6D_6) δ -3.2 ppm. **^{31}P{^{1}H} NMR** (243 MHz, C_6D_6) δ 34.21, -29.65 ppm. For $C_{74}H_{60}B_2N_2P_4$: C, 79.16; H, 5.39; N, 2.49 %. Found C, 78.89; H, 5.71; N, 3.05 %.

Theoretical Calculations

All calculations were performed using Orca 5.0.3, [59] using the PBE0 density functional,[60, 61] Grimme's D3 dispersion correction with Becke-Johnson damping,[62, 63] and the def2-SVP basis set[64] - labelled PBE0-D3(BJ)/def2-SVP. Geometries were optimized with the conductor-like polarizable continuum model (CPCM) for solvation with parameters for toluene.[65] The RIJCOSX approximation with a def2/J fitting set was employed for all calculations.[66] Minima were confirmed with vibration frequency calculations, performed analytically at the same level of theory. Transition state optimizations employed the NEB-TS approach.[67] All transition states were confirmed to connect relevant minima with intrinsic reaction coordinate (IRC) calculations.

ASSOCIATED CONTENT

Supporting Information.

The following files are available free of charge.

NMR Spectra, X-Ray Refinement Details, and Computational Details (file type, i.e., PDF)

Accession Codes

CCDC 2242925-2242939 contain the supplementary crystallographic data for this paper.[68] These data can be obtained free of charge via www.ccdc.cam.ac.uk/structures.

AUTHOR INFORMATION

Corresponding Authors

*** David J. D. Wilson -** Department of Chemistry, La Trobe Institute for Molecular Science, La Trobe University, Melbourne, 3086, Victoria, Australia; orcid.org/0000-0002-0007-4486; Email: david.wilson@latrobe.edu.au

*** Robert J. Gilliard, Jr**. - Department of Chemistry, Massachusetts Institute of Technology, 77 Massachusetts Avenue, Building 18-596, Cambridge, MA 02139-4307, United States; orcid.org/0000-0002-8830-1064; Email: gilliard@mit.edu

Author Contributions

Bi Youan Eric Tra - Department of Chemistry, Massachusetts Institute of Technology, 77 Massachusetts Avenue, Building 18-596, Cambridge, MA 02139-4307, United States; orcid.org/0000-0001-7441-4183

Andrew Molino - Department of Chemistry, La Trobe Institute for Molecular Science, La Trobe University, Melbourne, 3086, Victoria (Australia); orcid.org/0000-0002-0954-9054

Kimberly K. Hollister- Department of Chemistry, Massachusetts Institute of Technology, 77 Massachusetts Avenue, Building 18-596, Cambridge, MA 02139-4307, United States; orcid.org/0000-0001-9024-4436

Samir Kumar Sarkar- Department of Chemistry, Massachusetts Institute of Technology, 77 Massachusetts Avenue, Building 18-596, Cambridge, MA 02139-4307, United States; orcid.org/0000-0003-3822-6083

Diane A. Dickie - Department of Chemistry, University of Virginia, Charlottesville, Virginia 22904, United States; orcid.org/0000-0003-0939-3309

Notes

The authors declare no competing financial interest.

ACKNOWLEDGMENTS

The authors acknowledge the Massachusetts Institute of Technology, University of Virginia, and the National Science Foundation Chemical Synthesis (CHE-2046544) and Major Research Instrumentation (CHE-2018870) programs for support of this work. R.J.G. acknowledges additional laboratory support through a Beckman Young Investigator Award from the Arnold and Mabel Beckman Foundation. Generous allocation of computing resources from National Computational Infrastructure (NCI), Intersect, and La Trobe University are acknowledged.

References

1. Su, X.; Bartholome, T. A.; Tidwell, J. R.; Pujol, A.; Yruegas, S.; Martinez, J. J.; Martin, C. D., 9-Borafluorenes: Synthesis, Properties, and Reactivity. *Chem. Rev.* **2021**, *121*, 4147-4192.
2. Köster, R.; Benedikt, G., 9-Borafluorenes. *Angew. Chem., Int. Ed. Engl.* **1963**, *2*, 323-324.
3. He, J.; Rauch, F.; Finze, M.; Marder, T. B., (Hetero)arene-fused boroles: a broad spectrum of applications. *Chem. Sci.* **2021**, *12*, 128-147.
4. Steffen, A.; Ward, R. M.; Jones, W. D.; Marder, T. B., Dibenzometallacyclopentadienes, boroles and selected transition metal and main group heterocyclopentadienes: Synthesis, catalytic and optical properties. *Coord. Chem. Rev.* **2010**, *254*, 1950-1976.
5. Chen, X.; Meng, G.; Liao, G.; Rauch, F.; He, J.; Friedrich, A.; Marder, T. B.; Wang, N.; Chen, P.; Wang, S.; Yin, X., Highly Emissive 9-Borafluorene Derivatives: Synthesis, Photophysical Properties and Device Fabrication. *Eur. J. Chem.* **2021**, *27*, 6274-6282.
6. von Grotthuss, E.; John, A.; Kaese, T.; Wagner, M., Doping Polycyclic Aromatics with Boron for Superior Performance in Materials Science and Catalysis. *Asian J. Org. Chem.* **2018**, *7*, 37-53.
7. Ando, N.; Yamada, T.; Narita, H.; Oehlmann, N. N.; Wagner, M.; Yamaguchi, S., Boron-Doped Polycyclic π-Electron Systems with an Antiaromatic Borole Substructure That Forms Photoresponsive B–P Lewis Adducts. *J. Am. Chem. Soc.* **2021**, *143*, 9944-9951.
8. Zhang, C.; Wang, J.; Lin, Z.; Ye, Q., Synthesis, Characterization, and Properties of Three-Dimensional Analogues of 9-Borafluorenes. *Inorg. Chem.* **2022**, *61*, 18275-18284.
9. Bosdet, M. J. D.; Piers, W. E., B-N as a C-C substitute in aromatic systems. *Can. J. Chem.* **2009**, *87*, 8-29.
10. Frath, D.; Massue, J.; Ulrich, G.; Ziessel, R., Luminescent Materials: Locking π-Conjugated and Heterocyclic Ligands with Boron(III). *Angew. Chem. Int. Ed.* **2014**, *53*, 2290-2310.
11. Krantz, K. E.; Weisflog, S. L.; Frey, N. C.; Yang, W.; Dickie, D. A.; Webster, C. E.; Gilliard Jr., R. J., Planar, Stair-Stepped, and Twisted: Modulating Structure and Photophysics in Pyrene- and Benzene-Fused N-Heterocyclic Boranes. *Eur. J. Chem.* **2020**, *26*, 10072-10082.
12. Yang, D.-T.; Nakamura, T.; He, Z.; Wang, X.; Wakamiya, A.; Peng, T.; Wang, S., Doping Polycyclic Arenes with Nitrogen–Boron–Nitrogen (NBN) Units. *Org. Lett.* **2018**, *20*, 6741-6745.
13. Hertz, V. M.; Ando, N.; Hirai, M.; Bolte, M.; Lerner, H.-W.; Yamaguchi, S.; Wagner, M., Steric Shielding vs Structural Constraint in a Boron-Containing Polycyclic Aromatic Hydrocarbon. *Organometallics* **2017**, *36*, 2512-2519.
14. Hertz, V. M.; Massoth, J. G.; Bolte, M.; Lerner, H.-W.; Wagner, M., En Route to Stimuli-Responsive Boron-, Nitrogen-, and Sulfur-Doped Polycyclic Aromatic Hydrocarbons. *Eur. J. Chem.* **2016**, *22*, 13181-13188.
15. Miyamoto, F.; Nakatsuka, S.; Yamada, K.; Nakayama, K.-i.; Hatakeyama, T., Synthesis of Boron-Doped Polycyclic Aromatic Hydrocarbons by Tandem Intramolecular Electrophilic Arene Borylation. *Org. Lett.* **2015**, *17*, 6158-6161.
16. Dou, C.; Saito, S.; Matsuo, K.; Hisaki, I.; Yamaguchi, S., A Boron-Containing PAH as a Substructure of Boron-Doped Graphene. *Angew. Chem. Int. Ed.* **2012**, *51*, 12206-12210.
17. Liu, Z.; Marder, T. B., B-N versus C-C: how similar are they? *Angew. Chem. Int . Ed. Engl.* **2008**, *47*, 242-4.

18. Liu, Z.; Marder, T. B., B-N und C-C im Vergleich: Wie ähnlich sind sie einander?†. *Angewandte Chemie* **2008**, *120*, 248-250.
19. Rauch, F.; Fuchs, S.; Friedrich, A.; Sieh, D.; Krummenacher, I.; Braunschweig, H.; Finze, M.; Marder, T. B., Highly Stable, Readily Reducible, Fluorescent, Trifluoromethylated 9-Borafluorenes. *Eur. J. Chem.* **2020**, *26*, 12794-12808.
20. Krebs, J.; Häfner, A.; Fuchs, S.; Guo, X.; Rauch, F.; Eichhorn, A.; Krummenacher, I.; Friedrich, A.; Ji, L.; Finze, M.; Lin, Z.; Braunschweig, H.; Marder, T. B., Backbone-controlled LUMO energy induces intramolecular C–H activation in ortho-bis-9-borafluorene-substituted phenyl and o-carboranyl compounds leading to novel 9,10-diboraanthracene derivatives. *Chem. Sci.* **2022**, *13*, 14165-14178.
21. Escande, A.; Ingleson, M. J., Fused polycyclic aromatics incorporating boron in the core: fundamentals and applications. *Chem comm* **2015**, *51*, 6257-6274.
22. Wang, Z.; Zhou, Y.; Marder, T. B.; Lin, Z., DFT studies on reactions of boroles with carbon monoxide. *Organic & Biomolecular Chemistry* **2017**, *15*, 7019-7027.
23. He, J.; Rauch, F.; Friedrich, A.; Krebs, J.; Krummenacher, I.; Bertermann, R.; Nitsch, J.; Braunschweig, H.; Finze, M.; Marder, T. B., Phenylpyridyl-Fused Boroles: A Unique Coordination Mode and Weak B–N Coordination-Induced Dual Fluorescence. *Angew. Chem. Int. Ed.* **2021**, *60*, 4833-4840.
24. He, J.; Rauch, F.; Krummenacher, I.; Braunschweig, H.; Finze, M.; Marder, T. B., Two derivatives of phenylpyridyl-fused boroles with contrasting electronic properties: decreasing and enhancing the electron accepting ability. *Dalton Trans.* **2021**, *50*, 355-361.
25. Zhang, C.; Wang, J.; Su, W.; Lin, Z.; Ye, Q., Synthesis, Characterization, and Density Functional Theory Studies of Three-Dimensional Inorganic Analogues of 9,10-Diboraanthracene—A New Class of Lewis Superacids. *J. Am. Chem. Soc.* **2021**, *143*, 8552-8558.
26. Hertz, V. M.; Bolte, M.; Lerner, H.-W.; Wagner, M., Boron-Containing Polycyclic Aromatic Hydrocarbons: Facile Synthesis of Stable, Redox-Active Luminophores. *Angew. Chem. Int. Ed.* **2015**, *54*, 8800-8804.
27. Braunschweig, H.; Kupfer, T., Recent developments in the chemistry of antiaromatic boroles. *Chem comm* **2011**, *47*, 10903-10914.
28. Barnard, J. H.; Yruegas, S.; Huang, K.; Martin, C. D., Ring expansion reactions of anti-aromatic boroles: a promising synthetic avenue to unsaturated boracycles. *Chem comm* **2016**, *52*, 9985-9991.
29. Braunschweig, H.; Krummenacher, I.; Wahler, J., Chapter One - Free Boroles: The Effect of Antiaromaticity on Their Physical Properties and Chemical Reactivity. In *Advances in Organometallic Chemistry*, Hill, A. F.; Fink, M. J., Eds. Academic Press: 2013; Vol. 61, pp 1-53.
30. Zhang, W.; Zhang, B.; Yu, D.; He, G., Construction of highly antiaromatic boroles. *Sci. Bull.* **2017**, *62*, 899-900.
31. Snyder, J. A.; Grüninger, P.; Bettinger, H. F.; Bragg, A. E., Excited-State Deactivation Pathways and the Photocyclization of BN-Doped Polyaromatics. *J. Phys. Chem.* **2017**, *121*, 5136-5146.
32. Urban, M.; Durka, K.; Górka, P.; Wiosna-Sałyga, G.; Nawara, K.; Jankowski, P.; Luliński, S., The effect of locking π-conjugation in organoboron moieties in the structures of luminescent tetracoordinate boron complexes. *Dalton Trans.* **2019**, *48*, 8642-8663.
33. Iida, A.; Sekioka, A.; Yamaguchi, S., Heteroarene-fused boroles: what governs the antiaromaticity and Lewis acidity of the borole skeleton? *Chem. Sci.* **2012**, *3*, 1461-1466.

34. Shoji, Y.; Shigeno, N.; Takenouchi, K.; Sugimoto, M.; Fukushima, T., Mechanistic Study of Highly Efficient Direct 1,2-Carboboration of Alkynes with 9-Borafluorenes. *Eur. J. Chem.* **2018**, *24*, 13223-13230.
35. Berger, C. J.; He, G.; Merten, C.; McDonald, R.; Ferguson, M. J.; Rivard, E., Synthesis and Luminescent Properties of Lewis Base-Appended Borafluorenes. *Inorg. Chem.* **2014**, *53*, 1475-1486.
36. Mellerup, S. K.; Wang, S., Boron-Doped Molecules for Optoelectronics. *Trends in Chemistry* **2019**, *1*, 77-89.
37. Naveen, K. R.; Yang, H. I.; Kwon, J. H., Double boron-embedded multiresonant thermally activated delayed fluorescent materials for organic light-emitting diodes. *Communications Chemistry* **2022**, *5*, 149.
38. Yang, W.; Krantz, K. E.; Freeman, L. A.; Dickie, D. A.; Molino, A.; Frenking, G.; Pan, S.; Wilson, D. J. D.; Gilliard Jr., R. J., Persistent Borafluorene Radicals. *Angew. Chem. Int. Ed.* **2020**, *59*, 3850-3854.
39. Yang, W.; Krantz, K. E.; Freeman, L. A.; Dickie, D. A.; Molino, A.; Kaur, A.; Wilson, D. J. D.; Gilliard Jr., R. J., Stable Borepinium and Borafluorenium Heterocycles: A Reversible Thermochromic "Switch" Based on Boron–Oxygen Interactions. *Eur. J. Chem.* **2019**, *25*, 12512-12516.
40. Hollister, K. K.; Molino, A.; Breiner, G.; Walley, J. E.; Wentz, K. E.; Conley, A. M.; Dickie, D. A.; Wilson, D. J. D.; Gilliard, R. J., Jr., Air-Stable Thermoluminescent Carbodicarbene-Borafluorenium Ions. *J. Am. Chem. Soc.* **2022**, *144*, 590-598.
41. Wentz, K. E.; Molino, A.; Weisflog, S. L.; Kaur, A.; Dickie, D. A.; Wilson, D. J. D.; Gilliard Jr., R. J., Stabilization of the Elusive 9-Carbene-9-Borafluorene Monoanion. *Angew. Chem. Int. Ed.* **2021**, *60*, 13065-13072.
42. Wentz, K. E.; Molino, A.; Freeman, L. A.; Dickie, D. A.; Wilson, D. J. D.; Gilliard, R. J., Jr., Reactions of 9-Carbene-9-Borafluorene Monoanion and Selenium: Synthesis of Boryl-Substituted Selenides and Diselenides. *Inorg. Chem.* **2021**, *60*, 13941-13949.
43. Wentz, K. E.; Molino, A.; Freeman, L. A.; Dickie, D. A.; Wilson, D. J. D.; Gilliard, R. J., Jr., Activation of Carbon Dioxide by 9-Carbene-9-borafluorene Monoanion: Carbon Monoxide Releasing Transformation of Trioxaborinanone to Luminescent Dioxaborinanone. *J. Am. Chem. Soc.* **2022**, *144*, 16276-16281.
44. Wentz, K. E.; Molino, A.; Freeman, L. A.; Dickie, D. A.; Wilson, D. J. D.; Gilliard, R. J., Jr., Systematic Electronic and Structural Studies of 9-Carbene-9-Borafluorene Monoanions and Transformations into Luminescent Boron Spirocycles. *Inorg. Chem.* **2022**, *61*, 17049-17058.
45. Wentz, K. E.; Molino, A.; Freeman, L. A.; Dickie, D. A.; Wilson, D. J. D.; Gilliard Jr., R. J., Approaching Dianionic Tetraoxadiborecine Macrocycles: 10-Membered Bora-Crown Ethers Incorporating Borafluorenate Units. *Angew. Chem. Int. Ed. n/a*, e202215772.
46. Yang, W.; Krantz, K. E.; Dickie, D. A.; Molino, A.; Wilson, D. J. D.; Gilliard Jr., R. J., Crystalline BP-Doped Phenanthryne via Photolysis of The Elusive Boraphosphaketene. *Angew. Chem. Int. Ed.* **2020**, *59*, 3971-3975.
47. Biswas, S.; Oppel, I. M.; Bettinger, H. F., Synthesis and Structural Characterization of 9-Azido-9-Borafluorene: Monomer and Cyclotrimer of a Borole Azide. *Inorg. Chem.* **2010**, *49*, 4499-4506.
48. Müller, M.; Maichle-Mössmer, C.; Bettinger, H. F., BN-Phenanthryne: Cyclotetramerization of an 1,2-Azaborine Derivative. *Angew. Chem. Int. Ed.* **2014**, *53*, 9380-9383.

49. Keck, C.; Hahn, J.; Gupta, D.; Bettinger, H. F., Solution Phase Reactivity of Dibenzo[c,e][1,2]azaborinine: Activation and Insertion into Si-E Single Bonds (E=H, OSi(CH3)3, F, Cl) by a BN-Aryne. *Eur. J. Chem.* **2022**, *28*, e202103614.
50. Zhang, W.; Li, G.; Xu, L.; Zhuo, Y.; Wan, W.; Yan, N.; He, G., 9,10-Azaboraphenanthrene-containing small molecules and conjugated polymers: synthesis and their application in chemodosimeters for the ratiometric detection of fluoride ions. *Chem. Sci.* **2018**, *9*, 4444-4450.
51. Yruegas, S.; Martinez, J. J.; Martin, C. D., Intermolecular insertion reactions of azides into 9-borafluorenes to generate 9,10-B,N-phenanthrenes. *Chem comm* **2018**, *54*, 6808-6811.
52. Melen, R. L.; Lough, A. J.; Stephan, D. W., Boron azides in Staudinger oxidations and cycloadditions. *Dalton Trans.* **2013**, *42*, 8674-8683.
53. S. Nagai, T. H., S. Ogoshi and Y. Hoshimoto, N-Borane-Substituted Cyclic Phosphine Imides (BCPIs). *ChemRxiv* **2023**, preprint Febraury 20, 2023. DOI: 10.26434/chemrxiv-2023-qv422-v2
54. Courtenay, S.; Walsh, D.; Hawkeswood, S.; Wei, P.; Das, A. K.; Stephan, D. W., Boron and Aluminum Complexes of Sterically Demanding Phosphinimines and Phosphinimides. *Inorg. Chem.* **2007**, *46*, 3623-3631.
55. Hawkeswood, S.; Wei, P.; Gauld, J. W.; Stephan, D. W., Steric Effects in Metathesis and Reduction Reactions of Phosphinimines with Catechol- and Pinacolboranes. *Inorg. Chem.* **2005**, *44*, 4301-4308.
56. Holthausen, M. H.; Mallov, I.; Stephan, D. W., Phosphinimine-substituted boranes and borenium ions. *Dalton Trans.* **2014**, *43*, 15201-15211.
57. Bednarek, C.; Wehl, I.; Jung, N.; Schepers, U.; Bräse, S., The Staudinger Ligation. *Chem. Rev.* **2020**, *120*, 4301-4354.
58. Keck, C.; Hahn, J.; Gupta, D.; Bettinger, H. F., Solution Phase Reactivity of Dibenzo[c,e][1,2]azaborinine: Activation and Insertion into Si-E Single Bonds (E=H, OSi(CH3)3, F, Cl) by a BN-Aryne. *Eur. J. Chem. n/a.*
59. Neese, F., *WIREs Comput. Mol. Sci.* **2022**, e1606.
60. Perdew, J. P.; Ernzerhof, M.; Burke, K., Rationale for mixing exact exchange with density functional approximations. *J. Chem. Phys.* **1996**, *105*, 9982-9985.
61. Adamo, C.; Barone, V., Toward reliable density functional methods without adjustable parameters: The PBE0 model. *J. Chem. Phys.* **1999**, *110*, 6158-6170.
62. Grimme, S.; Antony, J.; Ehrlich, S.; Krieg, H., A consistent and accurate ab initio parametrization of density functional dispersion correction (DFT-D) for the 94 elements H-Pu. *J. Chem. Phys.* **2010**, *132*, 154104-1-154104-19.
63. Grimme, S.; Ehrlich, S.; Goerigk, L., Effect of the damping function in dispersion corrected density functional theory. *J. Comput. Chem.* **2011**, *32*, 1456-1465.
64. Weigend, F.; Ahlrichs, R., Balanced basis sets of split valence, triple zeta valence and quadruple zeta valence quality for H to Rn: Design and assessment of accuracy. *Phys. Chem. Chem. Phys.* **2005**, *7*, 3297-3305.
65. Barone, V.; Cossi, M., Quantum Calculation of Molecular Energies and Energy Gradients in Solution by a Conductor Solvent Model. *J. Phys. Chem.* **1998**, *102*, 1995-2001.
66. Neese, F.; Wennmohs, F.; Hansen, A.; Becker, U., Efficient, approximate and parallel Hartree–Fock and hybrid DFT calculations. A 'chain-of-spheres' algorithm for the Hartree–Fock exchange. *Chem. Phys.* **2009**, *356*, 98-109.

67. Ásgeirsson, V.; Birgisson, B. O.; Bjornsson, R.; Becker, U.; Neese, F.; Riplinger, C.; Jónsson, H., Nudged Elastic Band Method for Molecular Reactions Using Energy-Weighted Springs Combined with Eigenvector Following. *J Chem Theory Comput* **2021**, *17*, 4929-4945.
68. Tra, B. Y. E.; Molino, A.; Hollister, K. K.; Sarkar, S. K.; Dickie, D. A.; Wilson, D. J. D.; Gilliard Jr., R. J., Photochemically- and Thermally-Generated BN- and BNP-Doped Borafluorenate Heterocycles via Intramolecular Staudinger-Type Reactions. *ChemRxiv* **2023**, preprint February 21, 2023. DOI: 10.26434/chemrxiv-2023-71kvg

For Table of Contents Only

An array of new BN-containing heterocycles namely bis(borafluorene-phosphinimine)s have been synthesized via *intra*molecular Staudinger-type reactions assisted by diverse range of monodentate phosphine ligands. The reactions were initiated by heat or light with the extrusion of gaseous dinitrogen (N_2) molecule, and there was a migration of the phosphine ligand from boron center to nitrogen atom followed by dimerization resulting in bridges of two boron centers.